MITSUBISHI ELECTRIC RESEARCH LABORATORIES
http://www.merl.com

Optimal Signaling and Selection Verification for Single Transmit-Antenna Selection

Yabo Li, Neelesh Mehta, Andreas Molisch, Jinyun Zhang

TR2007-021 May 2007

Abstract

In marked contrast with the ideal error-free feedback assumption that is common in the literature, practical systems are likely to have severely bandwidth-limited, error-prone feedback channels. We consider the scenario where feedback from the receiver is used by the transmitter to select the best antenna, out of many available antennas, for data transmission. Feedback errors cause the transmitter to select an antenna different from the one signaled by the receiver. We show that optimizing the signaling assignment, which maps the antenna indices to the feedback codewords, improves performance without introducing any additional redundancy. For a system that uses error-prone feedback to transmit quadrature-phase-shift-keying-modulated data from a single antenna selected from many available spatially correlated antennas, we derive closed-form approximations for the data symbol error probability for an arbitrary number of receive antennas. We use these to systematically find the optimal signaling assignments using a low-complexity algorithm. The optimal signaling is intimately coupled to how the receiver performs selection verification, i.e., how it decodes the data signal when, due to feedback errors, it does not always know which antenna was used for data transmission. We show that ignoring feedback errors at the receiver can lead to an unacceptable performance degradation, and develop optimal and suboptimal, blind and nonblind selection-verification methods. With a small side-in-formation overhead, nonblind verification approaches the ideal perfect selection-verification performance.

IEEE Transactions on Communications

Optimal Signaling and Selection Verification for Single Transmit-Antenna Selection

Yabo Li, *Student Member, IEEE*, Neelesh B. Mehta, *Member, IEEE*, Andreas F. Molisch, *Fellow, IEEE*, and Jinyun Zhang, *Senior Member, IEEE*

***Abstract*—In marked contrast with the ideal error-free feedback assumption that is common in the literature, practical systems are likely to have severely bandwidth-limited, error-prone feedback channels. We consider the scenario where feedback from the receiver is used by the transmitter to select the best antenna, out of many available antennas, for data transmission. Feedback errors cause the transmitter to select an antenna different from the one signaled by the receiver. We show that optimizing the *signaling assignment*, which maps the antenna indices to the feedback codewords, improves performance without introducing any additional redundancy. For a system that uses error-prone feedback to transmit quadrature-phase-shift-keying-modulated data from a single antenna selected from many available spatially correlated antennas, we derive closed-form approximations for the data symbol error probability for an arbitrary number of receive antennas. We use these to systematically find the optimal signaling assignments using a low-complexity algorithm. The optimal signaling is intimately coupled to how the receiver performs *selection verification*, i.e., how it decodes the data signal when, due to feedback errors, it does not always know which antenna was used for data transmission. We show that ignoring feedback errors at the receiver can lead to an unacceptable performance degradation, and develop optimal and suboptimal, blind and nonblind selection-verification methods. With a small side-information overhead, nonblind verification approaches the ideal perfect selection-verification performance.**

***Index Terms*—Antenna arrays, antenna selection, combinatorial optimization, detection, diversity reception, maximum *a posteriori* (MAP) estimation, multiple-input multiple-output (MIMO) systems, radio receivers, receiving antennas, selection verification, spatial correlation, transmitting antennas.**

I. Introduction

While multiple-antenna systems promise remarkable improvements in the reliability of transmission over wireless channels, their widespread adoption has been inhibited by their increased hardware and signal complexity. Antenna selection, at the transmitter or receiver or both, is a low-complexity technique that reduces the hardware complexity of multiple-antenna systems [1]–[7] (tutorial articles can be found in [8]–[10]). By means of a selection switch, only a subset of the available antennas are used for data transmission or reception. Therefore, fewer RF chains than the number of antennas are required. While more than one antenna can be selected in general, single transmit-antenna selection is beneficial, as it retains the full diversity order in a frequency-flat block-fading channel [6], [7].[1] It enables the use of conventional single-input single-output transmission schemes while also exploiting spatial diversity.

Feedback is critical in implementing transmit-antenna selection (TAS), as channel state information (CSI) is often not readily available at the transmitter. However, in practical systems, the feedback channel is typically severely bandwidth-limited and designed with a tight link budget. For example, in third-generation (3G) cellular systems [11], the feedback is uncoded and its rate is just 1.5 kb/s. Feedback bit-error rates (BERs) as high as 4% are not uncommon. While error-correction coding can be used to reduce this error rate, the extra bits required increase the feedback latency and reduce the maximum Doppler frequency that the system can handle. The above scenario is in marked contrast with the ideal error-free feedback that is typically assumed in the literature on selection [4], [12]–[14].

Feedback errors can cause the antenna selected by the transmitter to be different from the optimum one requested by the receiver. If the large difference between the feedback BER (on the reverse link) and the desired data BER (on the forward link), which is as low as 10^{-4}, is ignored, it can significantly increase the data BER actually achieved. Another factor that affects the performance of selection is spatial correlation between the transmit antennas. The correlation depends not only on the antenna topology, but also the wireless propagation environment [15]–[19]. The combined impact of both these effects needs to be jointly compensated to minimize the performance degradation; if not, the degradation can often be unacceptable.

Feedback nonidealities were modeled in [12] and [20]–[22]. However, [20] considers only three transmit antennas and provides only simulation results. It also assumes that in case of a feedback error, any of the candidate antennas is used by the transmitter with equal probability. Under this assumption, all signaling assignments, which determine the assignment of feedback codewords to the antennas to be used for transmission, give exactly the same performance, which, as we shall see, is not the case. The same idealized assumption about receiver knowledge

Paper approved by M.-S. Alouini, the Editor for Modulation and Diversity Systems of the IEEE Communications Society. Manuscript received August 26, 2005; revised April 10, 2006 and July 7, 2006. This paper was presented in part at the IEEE Global Telecommunications Conference, San Francisco, CA, 2006.

Y. Li was with Mitsubishi Electric Research Labs (MERL), Cambridge, MA 02139 USA. He is now with the System Design Group, Nortel Networks, Richardson, TX 75082 USA (e-mail: yaboli@nortel.com).

N. B. Mehta and J. Zhang are with Mitsubishi Electric Research Labs (MERL), Cambridge, MA 02139 USA (e-mail: mehta@merl.com; jzhang@merl.com).

A. F. Molisch is with Mitsubishi Electric Research Labs (MERL), Cambridge, MA 02139 USA, and is also with Lund University, Lund, Sweden (e-mail: molisch@merl.com).

Digital Object Identifier 10.1109/TCOMM.2007.892461

[1]In general, when multiple antennas are selected, full diversity may not be retained if the space–time trellis code (STTC) used is rank-deficient or the channel undergoes fast fading.

is also made in [12] and [21]. All the above papers also assumed that the receiver somehow always knows what antenna(s) were used for transmission, which is clearly an idealization. While [22] considers feedback delay in closed-loop transmit-diversity systems, it does not assume feedback errors.

The contributions of the paper are the following. For a system with N_r receive antennas that selects one antenna from N_t spatially correlated transmit antennas and operates with an error-prone feedback (reverse) channel, we show how the feedback signaling design affects the average symbol-error probability (SEP). We develop a systematic, low-complexity method for determining the optimal signaling assignment. This is crucial, as the number of signaling assignments grows as $O(N_t!)$, which makes a brute-force search practically infeasible. The optimal signaling assignment turns out to be intimately coupled with the receiver design. We then develop novel receiver designs for antenna selection to deal with imperfect feedback, which we call *antenna selection verification*. As the performance degradation without verification is often unacceptable, and perfect verification is an idealization, we develop and evaluate several selection-verification algorithms such as symbol-level and block-level *blind algorithms*, in which the receiver uses the received (but unknown) data and its *a priori* channel knowledge to estimate the transmit-antenna set used, and *nonblind algorithms*, which are aided by additional side information.

To our knowledge, feedback signaling in a spatially correlated multiple-antenna data channel, as well as the receiver design problem, have not been studied in the literature. One reason for this is the analytical intractability of this seemingly simple problem. Elegant analytical techniques such as virtual branch combining [23], [24, Ch. 9], which is based on order statistics of independent antenna gains, are not available if the channel is correlated. Therefore, the resultant analysis is significantly complicated [25]. Feedback errors further complicate the analysis. However, the simple closed-form analytical approximations developed in this paper overcome this hurdle, at least for finding the optimal signaling assignment.

The paper is organized as follows. Section II mathematically formulates the problem of antenna-selection signaling. Section III derives the performance metric related to SEP. The algorithm for determining the best feedback signaling assignment is developed in Section IV. Antenna selection-verification methods are discussed in Section V. Section VI presents the numerical results, and Section VII presents our conclusions.

II. System Model

Notation: The symbol $(.)^T$ denotes matrix transpose, $(.)^\dagger$ the Hermitian transpose, $||.||$ the norm of a vector, and $||.||_F$ the Frobenious norm. The symbol $\mathbb{C}^{a\times b}$ denotes the set of $a \times b$ complex matrices. $\mathbb{E}_{A|B}[.]$ denotes the expectation over the random variable (RV) A given B. Similarly, $\Pr(A|B)$ denotes the conditional probability of A given B if A is a discrete RV, and $p(A|B)$ denotes the probability density function (pdf) of A given B if A is a continuous RV.

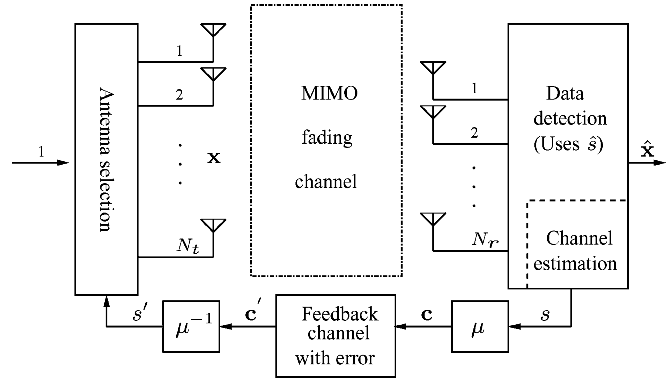

Fig. 1. Schematic of TAS with erroneous feedback.

Fig. 1 shows our system model. From N_t transmit antennas, one is selected. There are N_r antennas at the receiver. The received signal vector $\mathbf{y} \triangleq [y_1, y_2, \cdots, y_{N_r}]^T \in \mathbb{C}^{N_r\times 1}$ is

$$\mathbf{y} = \mathbf{h}_j x + \mathbf{w} \tag{1}$$

where x is the transmitted quaternary phase-shift keying (QPSK) symbol, $\mathbf{w}$ is the additive white complex Gaussian noise (AWCGN) vector with independent and identically distributed (i.i.d.) zero-mean unit-variance elements. The complex vector $\mathbf{h}_j$ is the jth column of the complete channel matrix $\mathbf{H}$, where j is the index of the antenna used for transmission. The matrix $\mathbf{H} \in \mathbb{C}^{N_r\times N_t}$ consists of all the channel coefficients between the transmitter and the receiver. The signal-to-noise ratio (SNR) is denoted by γ, where $\gamma = \mathbb{E}_x[|x|^2]$.

As per the Kronecker model, which models well several typical spatial channels, the forward channel matrix $\mathbf{H}$ can be written as [17], [19]

$$\mathbf{H} = \mathbf{R}_r^{1/2}\mathbf{H}_w\mathbf{R}_t^{1/2} \tag{2}$$

where $\mathbf{R}_t$ is the $N_t \times N_t$ transmit-side correlation matrix, $\mathbf{R}_r$ is the $N_r \times N_r$ receive-side correlation matrix, and $\mathbf{H}_w$ is an $N_r \times N_t$ spatially white zero-mean unit variance complex i.i.d. Gaussian noise matrix. The spatial covariance matrices for a uniform linear array (ULA) with a Gaussian angle spread and a uniform circular array (UCA) with a Laplacian angle spread are derived in [19] and [26], respectively. They depend on the angular power spectrum, in particular, the angle spread, σ_θ, the mean angle of departure/arrival (AoD/AoA), θ_0, and the wavelength-normalized antenna spacing Δ for a ULA, or the wavelength-normalized array radius Ω for a UCA.

A. Notation for TAS Signaling

To minimize overhead, the receiver does not feed back the entire channel state, but only computes and feeds back the indices of the antenna that the transmitter must use. Let $\mathcal{S}$ denote the set of all possible single transmit antenna choices, $\mathcal{S} \triangleq \{1, 2, \ldots, N_t\}$.[2] To make the transmitter use the antenna s, the receiver sends the feedback codeword (bit sequence) $\mathbf{c} \triangleq [c_1, c_2, \ldots, c_n] \in \mathbb{F}^n$, where $\mathbb{F} \triangleq \{0, 1\}$. Let $\mathcal{C}$ denote

[2]To keep the discussion concise, we no longer distinguish between the antennas and their indices.

the set of all feedback codewords (the used bit sequences), $\mathcal{C} \triangleq \{\mathbf{c}_1, \mathbf{c}_2, \dots, \mathbf{c}_{N_t}\}$. All the codewords consist of n bits. Such feedback is needed whenever the short-term fading in the forward and reverse channels is uncorrelated, as is typically the case in frequency-division duplex systems, or in time-division duplex systems with asymmetric forward and reverse links, or in high Doppler regimes.

To ensure meaningful feedback, each of the N_t possible choices must be represented by a unique bit sequence. Therefore, the length of the bit sequences, n, satisfies the constraint $n \geq \lceil \log_2 N_t \rceil$, where $\lceil \cdot \rceil$ is the ceiling function. For simplicity, N_t is taken to be a power of 2, so that the total number of possible bit sequences and the number of antennas is the same, i.e., $n = \log_2 N_t$ is an integer.[3] Therefore, there exists a bijective mapping μ, $\mathcal{S} \mapsto \mathcal{C}$, called the *signaling assignment*, such that for any codeword $\mathbf{c} \in \mathcal{C}$, there exists a transmit antenna $s \in \mathcal{S}$ such that $\mathbf{c} = \mu(s)$, and no two transmit antennas are assigned the same codeword, $\mu(s_1) \neq \mu(s_2)$ for any $s_1 \neq s_2$.

B. Feedback Channel Model and Its Impact

TAS with erroneous feedback can be described as follows. Let s denote the optimum choice made by the receiver. The receiver signals the codeword $\mathbf{c} = \mu(s)$, which is received by the transmitter as $\mathbf{c}'$. The transmitter then uses the antenna set $s' = \mu^{-1}(\mathbf{c}')$. Given that $\mu(.)$ is bijective, it follows that $s \neq s'$ if $\mathbf{c} \neq \mathbf{c}'$.

Errors in the feedback channel result in the transmitter receiving a bit sequence $\mathbf{c}'$ that is different from the one sent by the receiver, $\mathbf{c}$. Let ϵ denote the probability that a feedback bit changes from 0 to 1 or vice versa. The probability of confusing these two bit sequences is given by the function

$$\Phi(d) = \epsilon^d (1-\epsilon)^{n-d} \tag{3}$$

where d is the Hamming distance between two feedback bit sequences. Thus, different Hamming distances lead to different error probabilities.

C. Notation for Antenna-Selection Verification

Throughout this paper, we shall assume that the receiver knows $\mathbf{H}$, for example, by initial training.[4] Due to the presence of feedback errors, the receiver does not know *a priori* the antenna actually used for transmission. To fulfill its ultimate goal of detecting the transmission data correctly, the receiver often needs to estimate, as an intermediate step, which antenna was used by the transmitter. This process is called *antenna-selection verification*, given its resemblance to a problem that occurs in closed-loop transmit-diversity systems with imperfect transmit weight feedback [27]–[29]. Hereafter, we use s, s', and $\hat{s}$ to denote the antennas chosen (and fed back) by the receiver, actually used by the transmitter, and assumed by the receiver during data detection, respectively. Their corresponding channel gain vectors, which correspond to appropriate columns of the complete channel matrix $\mathbf{H}$, are denoted by $\mathbf{h}_s$, $\mathbf{h}_{s'}$, and $\mathbf{h}_{\hat{s}}$.

A receiver that ignores the possibility of feedback errors and assumes that the transmitter used the antenna s recommended by the receiver, is called the *no-selection verification receiver*. It therefore assumes that $\hat{s} = s$ and uses the channel $\mathbf{h}_s$ to do detection. On the other hand, if the receiver always knows, say, with the help of a genie, that the antenna s' was used by the transmitter, it shall be called the *perfect selection-verification receiver*. It therefore assumes $\hat{s} = s'$ and correctly uses $\mathbf{h}_{s'}$ to do detection. A receiver that determines $\hat{s}$ using only the received signal $\mathbf{y}$, given *a priori* knowledge of the feedback error rate ϵ, is called the *blind selection-verification receiver*. If, as discussed later, additional side information is also available to determine $\hat{s}$, we shall call it the *nonblind selection-verification receiver*.

To quantify the efficacy of the selection-verification algorithms and understand their behavior, we define two verification-related probabilities

selection verification error probability:

$$P^{(E)} \triangleq \Pr(\hat{s} \neq s') \tag{4}$$

selection verification mismatch probability:

$$P^{(M)} \triangleq \Pr(\hat{s} \neq s). \tag{5}$$

$P^{(E)}$ is the probability that the receiver cannot determine which transmit antenna was actually used. $P^{(M)}$ is the probability that the transmit-antenna estimate at the receiver does not match its initial (optimum) choice. Obviously, $P^{(E)} = 0$ for perfect selection verification, and $P^{(M)} = 0$ for no-selection verification.[5]

III. Signaling Assignment: Optimization Metrics

In the previous section, we saw that not all feedback codeword errors are equally likely. In the absence of spatial correlation, the average SEP of the data is independent of the signaling assignment. However, in the presence of correlation, it can be intuitively seen that the performance degradation can be reduced if the signaling assignment ensures that the antenna actually used is correlated with the antennas the receiver signals the transmitter to use.

To verify this intuition, a toy example of a ULA consisting of $N_t = 4$ antennas with $N_r = 1$ is illustrated in Fig. 2. The total number of possible signaling assignments, when two feedback bits are used, is $4! = 24$, which makes brute-force Monte Carlo simulations feasible. We plot the average SEP as a function of the SNR for each and every signaling assignment. The performance for two feedback BERs, $\epsilon = 0.1\%$ and $\epsilon = 4\%$, is shown for both the ideal perfect selection-verification receiver, which always knows which antenna was actually used by the transmitter, and the no-selection-verification receiver, which ignores feedback errors and assumes that the transmitter used the

[3] If N_t is not a power of two, there will exist for the uncoded feedback case $2^n - N_t$ bit sequences that are not codewords. When the transmitter receives them due to feedback errors, it maps them to transmit antennas using a prespecified rule. We do not delve into this issue in this paper.

[4] It must be noted that the training duration is longer because not all antennas can be trained over simultaneously in an antenna-selection system with fewer RF chains. For the same block-fading duration, this leads to a shorter duration for data transmission.

[5] The formalism defined so far for single TAS can be easily generalized to the case of hybrid selection, in which a subset containing more than one transmit antenna is selected. The set $\mathcal{S}$ now contains vectors $\mathcal{S} = \{\mathbf{s}_1, \dots, \mathbf{s}_L\}$, where each vector $\mathbf{s}_i$ has as its elements the selected antennas. The number of choices L is now $\binom{N_t}{\mathcal{L}_t}$, if $\mathcal{L}_t$ antennas are always chosen. The received signal becomes $\mathbf{y} = \tilde{\mathbf{H}}\mathbf{x} + \mathbf{w}$, where the vector $\mathbf{x}$ is the data transmitted from the selected antennas and the matrix $\tilde{\mathbf{H}}$ is the corresponding subset of $\mathbf{H}$.

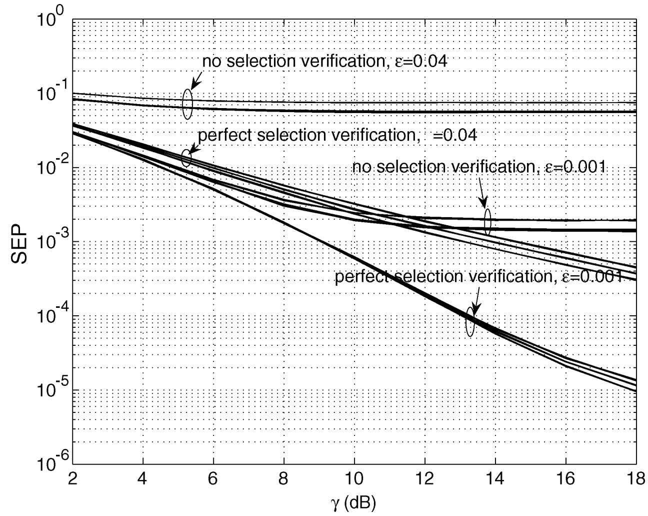

Fig. 2. Data SEP for all 24 signaling assignments for no-selection-verification and perfect selection-verification receivers (ULA, $N_t = 4$, $N_r = 1$). Results are shown for two feedback BERs: $\epsilon = 4\%$ and $\epsilon = 0.1\%$.

antenna recommended by the receiver. The transmit correlation matrix corresponds to an angle spread of $\sigma_\theta = 30^\circ$ and a mean AoD of 30°. The performance gap between the best and the worst signaling assignments is about 1.5 dB for perfect selection verification. And for no-selection verification, the best and the worst signaling assignments both suffer from an error floor which is on the order of $n\epsilon$. While the performance loss is negligible for $\epsilon = 0.1\%$ (except at high SNR), it is significant for $\epsilon = 4\%$.

We now develop the analysis to find the optimal signaling assignment systematically without resorting to arduous brute-force simulations. Let $\mathcal{M}_{N_t}$ denote the set of all signaling assignments (bijective mappings between two sets of cardinality N_t). Then the optimal signaling assignment, μ^*, for a given SNR γ is

$$\mu^*(\gamma) = \arg \min_{\mu \in \mathcal{M}_{N_t}} P_e(\mu; \gamma) \tag{6}$$

where $P_e(\mu; \gamma)$ denotes the average SEP for the signaling assignment μ at SNR γ. Arguably, while the optimal assignment, μ^*, can depend on the operating γ, the results in Fig. 2 (and others in later sections) show that for perfect selection verification and no-selection verification, the same signaling assignment is optimal for all SNRs. For other receivers, this might not be true, as we shall see in later sections.

When one transmit antenna is selected from the N_t antennas, the optimal transmit antenna choice is

$$\mathbf{s} = \arg \max_j \|\mathbf{h}_j\|^2 \tag{7}$$

where $\mathbf{h}_j$ denotes the jth column of $\mathbf{H}$. The decision statistic used by the receiver, given that it uses $\hat{s}$ as its estimate of the antenna used for transmission and knows $\mathbf{H}$, is

$$\hat{y} = \mathbf{h}_{\hat{s}}^\dagger y = \mathbf{h}_{\hat{s}}^\dagger \mathbf{h}_{s'} x + \mathbf{h}_{\hat{s}}^\dagger \mathbf{w}. \tag{8}$$

The output of the detector is denoted by $\hat{x}$.

The average SEP for a given signaling assignment μ is

$$P_e(\mu; \gamma) = \sum_{s, s', \hat{s} \in \mathcal{S}} \mathbb{E}_{x|s,s',\hat{s}} \left[\Pr(\hat{x} \neq x | s, s', \hat{s})\right] \times \Pr(\hat{s}|s, s') \Pr(s'|s) \Pr(s).$$

The probability $\Pr(\hat{s}|s', s)$ depends on the selection-verification algorithm used at the receiver. For perfect selection verification, we have $\Pr(\hat{s} = s'|s', s) = 1$, while for no-selection verification, $\Pr(\hat{s} = s|s', s) = 1$. Therefore, in these two cases, in which $\hat{s}$ is a deterministic function of s and s', the above equation can be simplified to

$$P_e(\mu; \gamma) = \sum_{s, s' \in \mathcal{S}} \mathbb{E}_{x|s,s'} \left[\Pr(\hat{x} \neq x | s, s')\right] \Pr(s'|s) \Pr(s). \tag{9}$$

The term $\Pr(s'|s)$ depends on the feedback BER ϵ and the signaling assignment μ because

$$\Pr(s'|s) = \Phi\left(d(\mathbf{c}', \mathbf{c})\right) = \epsilon^{d(\mathbf{c}', \mathbf{c})} (1 - \epsilon)^{\left(n - d(\mathbf{c}', \mathbf{c})\right)} \tag{10}$$

where $\mathbf{c}' = \mu(s')$, $\mathbf{c} = \mu(s)$, and $d(\mathbf{c}, \mathbf{c}')$ denotes the Hamming distance between the two codewords $\mathbf{c}$ and $\mathbf{c}'$. $\Pr(s)$ is the probability that s is the optimal transmit antenna. In the presence of spatial correlation, it is not necessarily the same for all s. However, for moderate spatial correlations, the difference between these probabilities is minor enough to justify the approximation $\Pr(s) \approx 1/N_t$. For example, when a ULA consists of $N_t = 4$ antennas with $\Delta = 0.5$, $\sigma_\theta = 30^\circ$, and $\theta_0 = 30^\circ$, we have $\Pr(s = 1) = \Pr(s = 4) = 0.28$, $\Pr(s = 2) = \Pr(s = 3) = 0.22$.

We then get the following expression for $P_e(\mu; \gamma)$:

$$P_e(\mu; \gamma) \approx \frac{1}{N_t} \sum_{s, s'} \mathbb{E}_{x|s,s'} [\Pr(\hat{x} \neq x | s, s')] \Phi(d\left(\mu(s'), \mu(s)\right)). \tag{11}$$

The average SEP given s and s', $\mathbb{E}_{x|s,s'}[\Pr(\hat{x} \neq x | s, s')]$, depends on the modulation constellation, the receiver, and the channel statistics. The combination of spatial correlation, order statistics, and feedback errors makes it difficult to derive general closed-form expressions for the above expectation. Evaluating it numerically or using Monte Carlo simulations is infeasible for optimization purposes, as the entire SEP curve (as a function of SNR) needs to be plotted for every signaling assignment. We therefore develop simple closed-form approximations for the SEP that are based only on the second-order statistics of the channel. These are shown to be sufficiently accurate for optimizing the signaling assignment.

A. *Closed-Form SEP Approximation for Perfect Selection Verification*

With perfect antenna-selection verification, we have $\hat{s} = s'$. Therefore, the decision statistic becomes

$$\hat{y} = \|\mathbf{h}_{s'}\|^2 x + \mathbf{h}_{s'}^\dagger \mathbf{w}. \tag{12}$$

When QPSK modulation is used, the SEP, given $\mathbf{h}_{s'}$, approximately equals $2Q(\sqrt{\gamma\|\mathbf{h}_{s'}\|^2/2})$. Therefore

$$\Pr(\hat{x}\neq x|s,s') = \mathbb{E}_{\mathbf{h}_{s'}|s,s'}\left[2Q\left(\sqrt{\frac{\gamma}{2}\|\mathbf{h}_{s'}\|^2}\right)\right] \tag{13}$$

$$\approx 2Q\left(\sqrt{\frac{\gamma}{2}\mathbb{E}_{\mathbf{h}_{s'}|s,s'}\left[\|\mathbf{h}_{s'}\|^2\right]}\right). \tag{14}$$

In (14), we interchanged the expectation operator and the Q function. From Jensen's inequality, the resulting expression is a lower bound on the average SEP.

From the spatial correlation model defined in (2), the correlation between $\mathbf{h}_{s'}$ and $\mathbf{h}_s$ is $r_{ss'}$. Then, $\mathbf{h}_{s'}$ can be written in terms of $\mathbf{h}_s$ as $\mathbf{h}_{\hat{s}} = r_{ss'}\mathbf{h}_s + \sqrt{1-|r_{ss'}|^2}\mathbf{n}$. The vector $\mathbf{n}$ is independent of $\mathbf{h}_{\hat{s}}$ and $\mathbf{h}_s$, and each of its elements is a zero-mean unit-variance complex Gaussian RV. Therefore, $\mathbb{E}_{\mathbf{h}_{s'}|s,s'}[\|\mathbf{h}_{s'}\|^2] = |r_{ss'}|^2\mathbb{E}_{\mathbf{h}_s|s}[\|\mathbf{h}_s\|^2] + (1-|r_{ss'}|^2)N_r$. Therefore

$$\begin{aligned}\Pr(\hat{x}\neq x|s,s') &\approx 2Q\left(\sqrt{\frac{\gamma}{2}|r_{ss'}|^2\left(\mathbb{E}_{\mathbf{h}_s|s}\left[\|\mathbf{h}_s\|^2\right]-N_r\right)+\frac{N_r\gamma}{2}}\right)\\ &\approx 2\exp\left(-\frac{\gamma}{4}|r_{ss'}|^2\left(\mathbb{E}_{\mathbf{h}_s|s}\left[\|\mathbf{h}_s\|^2\right]-N_r\right)-\frac{N_r\gamma}{4}\right) \quad (15)\\ &= 2\exp\left(-\beta_{\mathrm{ver}}(\gamma)|r_{ss'}|^2\right)\exp\left(-\frac{N_r\gamma}{4}\right). \quad (16)\end{aligned}$$

In (15), we used the approximation $Q(a)\approx\exp(-a^2/2)$, for $a>0$. The term $\beta_{\mathrm{ver}}(\gamma)$ in (16) denotes $(\gamma/4)(\mathbb{E}_{\mathbf{h}_s|s}[\|\mathbf{h}_s\|^2]-N_r)$, as $\mathbb{E}_{\mathbf{h}_s|s}[\|\mathbf{h}_s\|^2]$ is independent of μ. It must be noted that $\beta_{\mathrm{ver}}(\gamma)>0$, because $\|\mathbf{h}_s\|^2$ is the maximum of the column norms of $\mathbf{H}$.

Since x is QPSK-modulated and the constellation symbols are equiprobable, we have $\mathbb{E}_{x|s,s'}[\Pr(\hat{x}\neq x|s,s')] = \Pr(\hat{x}\neq x|s,s')$. Substituting the expressions for $\Pr(\hat{x}\neq x|s,s')$ from (16), and for $\Phi(.)$ from (3), in (9), we get the following expression for $P_e(\mu;\gamma)$:

$$P_e(\mu;\gamma)\approx\frac{2}{N_t}\exp\left(-\frac{N_r\gamma}{4}\right)(1-\epsilon)^n \times\sum_{s\in\mathcal{S}}\sum_{s'\in\mathcal{S}}\exp\left(-\beta_{\mathrm{ver}}(\gamma)|r_{ss'}|^2\right)\left(\frac{\epsilon}{1-\epsilon}\right)^{d\left(\mu(s),\mu(s')\right)}. \tag{17}$$

Therefore, the SEP metric $M_{\mathrm{ver}}(\mu;\gamma)$ to be optimized for perfect selection verification can be defined as

$$M_{\mathrm{ver}}(\mu;\gamma)\triangleq\sum_{s\in\mathcal{S}}\sum_{s'\in\mathcal{S}}\exp\left(-\beta_{\mathrm{ver}}(\gamma)|r_{ss'}|^2\right)\times\left(\frac{\epsilon}{1-\epsilon}\right)^{d\left(\mu(s),\mu(s')\right)}. \tag{18}$$

The common term $(2/N_t)\exp(-(N_r\gamma/4))(1-\epsilon)^n$, which does not depend on μ, is dropped in (18).

B. Closed-Form SEP Approximation for No-Selection Verification

A receiver that does not do antenna selection verification uses $\hat{s}=s$. Therefore, the decision statistic in this receiver is

$$\hat{y}=\mathbf{h}_s^\dagger\mathbf{h}_{s'}x+\mathbf{h}_s^\dagger\mathbf{w}. \tag{19}$$

Therefore, when x is QPSK-modulated, we have

$$\begin{aligned}\Pr(\hat{x}\neq x|s,s') &= \mathbb{E}_{\mathbf{h}_{s'},\mathbf{h}_s|s,s'}\left[\Pr(\hat{x}\neq x|\mathbf{h}_{s'},\mathbf{h}_s,s,s')\right]\\ &= \mathbb{E}_{\mathbf{h}_{s'},\mathbf{h}_s|s,s'}\left[Q\left(\sqrt{\frac{\gamma}{2}}\frac{|\mathbf{h}_s^\dagger\mathbf{h}_{s'}|}{\|\mathbf{h}_s\|}\cos\left(\frac{\pi}{4}+\phi\right)\right)\right.\\ &\qquad\left.+Q\left(\sqrt{\frac{\gamma}{2}}\frac{|\mathbf{h}_s^\dagger\mathbf{h}_{s'}|}{\|\mathbf{h}_s\|}\sin\left(\frac{\pi}{4}+\phi\right)\right)\right]\end{aligned}$$

where ϕ is the phase of the complex number $\mathbf{h}_s^\dagger\mathbf{h}_{s'}$. It is a zero-mean RV, and its variance decreases as the spatial correlation increases. For small ϕ, we have $|\sin(\phi)|\ll|\cos(\phi)|$. This justifies the following approximation: $\cos((\pi/4)+\phi) = (1/\sqrt{2})\cos(\phi)-(1/\sqrt{2})\sin(\phi)\approx(1/\sqrt{2})\cos(\phi)$. Similarly, $\sin((\pi/4)+\phi)\approx(1/\sqrt{2})\cos(\phi)$. Therefore

$$\Pr(\hat{x}\neq x|\mathbf{h}_{s'},\mathbf{h}_s,s,s')\approx 2Q\left(\sqrt{\frac{\gamma}{4}}\frac{|\mathbf{h}_s^\dagger\mathbf{h}_{s'}|}{\|\mathbf{h}_s\|}\cos(\phi)\right). \tag{20}$$

As before, the spatial correlation between $\mathbf{h}_s$ and $\mathbf{h}_{s'}$ implies that $\mathbf{h}_{s'} = r_{ss'}\mathbf{h}_s + \sqrt{1-|r_{ss'}|^2}\mathbf{n}$. Thus, we have $|\mathbf{h}_s^\dagger\mathbf{h}_{s'}|\cos(\phi) = \|\mathbf{h}_s\|^2\mathrm{Re}\{r_{ss'}\} + \mathrm{Re}\{\sqrt{1-|r_{ss'}|^2}\mathbf{h}_s^\dagger\mathbf{n}\}$, where $\mathbf{n}$ is a zero-mean AWCGN and is independent of $\mathbf{h}_s$ and $\mathbf{h}_{s'}$. Therefore

$$\Pr(\hat{x}\neq x|\mathbf{h}_{s'},\mathbf{h}_s,s,s') \approx 2Q\left(\sqrt{\frac{\gamma}{4}}\|\mathbf{h}_s\|\mathrm{Re}\{r_{ss'}\}+\mathrm{Re}\left\{\sqrt{1-|r_{ss'}|^2}\frac{\mathbf{h}_s^\dagger\mathbf{n}}{\|\mathbf{h}_s\|}\right\}\right). \tag{21}$$

Then $\Pr(\hat{x}\neq x|s,s')$ can be approximated by

$$\begin{aligned}\Pr(\hat{x}\neq x|s,s') &\approx 2Q\left(\sqrt{\frac{\gamma}{4}}\mathbb{E}_{\mathbf{h}_{s'}|s,s'}\left[\|\mathbf{h}_s\|\right]\mathrm{Re}\{r_{ss'}\}\right)\\ &= 2Q\left(\beta_{\mathrm{no-ver}}(\gamma)\mathrm{Re}\{r_{ss'}\}\right). \quad (22)\end{aligned}$$

The first step of the approximation swaps the expectation operator and the Q function. From Jensen's inequality, the resulting expression is a lower bound on the average SEP. This step also uses the fact that $\mathbb{E}_{\mathbf{h}_s,\mathbf{n}|s,s'}[\mathrm{Re}\{\sqrt{1-|r_{ss'}|^2}(\mathbf{h}_s^\dagger\mathbf{n}/\|\mathbf{h}_s\|)\}]=0$ because $\mathbf{n}$ is a zero-mean RV that is independent of $\mathbf{h}_s$. In (22), $\beta_{\mathrm{no-ver}}(\gamma)$ denotes $\sqrt{(\gamma/4)}\mathbb{E}_{\mathbf{h}_{s'}|s,s'}[\|\mathbf{h}_s\|]$, which is independent of μ. Note the approximation $Q(a)\approx\exp(-a^2/2)$, which we had used earlier, is unsuitable here because $\mathrm{Re}\{r_{ss'}\}$ can be negative.

Upon substituting (22) and (3) in (11), we get

$$P_e(\mu;\gamma)\approx\frac{2}{N_t}(1-\epsilon)^n\sum_{s\in\mathcal{S}}\sum_{s'\in\mathcal{S}}Q\left(\beta_{\mathrm{no-ver}}(\gamma)\mathrm{Re}\{r_{ss'}\}\right)\times\left(\frac{\epsilon}{1-\epsilon}\right)^{d\left(\mu(s'),\mu(s)\right)}. \tag{23}$$

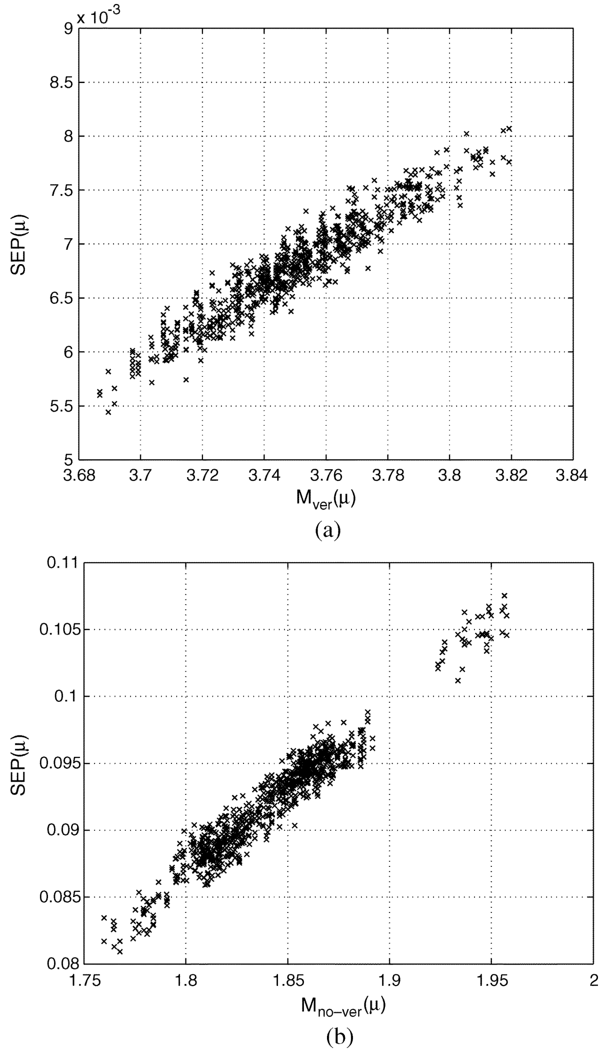

Fig. 3. Scatter plot showing the monotonic relationship between $M(\mu;\gamma)$, which approximates the average SEP, and the numerically computed average SEP for different signaling assignments μ, for single antenna selection with the SNR fixed at $\gamma = 6$ dB ($N_t = 8$, $N_r = 1$). (a) Perfect selection verification. (b) No-selection verification.

Therefore, we can define the SEP metric $M_{\text{no-ver}}(\mu;\gamma)$ for no-selection verification as

$$M_{\text{no}-\text{ver}}(\mu;\gamma) \triangleq \sum_{s\in\mathcal{S}}\sum_{s'\in\mathcal{S}} Q\left(\beta_{\text{no}-\text{ver}}(\gamma)\text{Re}\{r_{ss'}\}\right) \times \left(\frac{\epsilon}{1-\epsilon}\right)^{d\left(\mu(s'),\mu(s)\right)}. \quad (24)$$

The common term $(2/N_t)(1-\epsilon)^n$, which is independent of μ, is dropped in the above definition.

C. Validation of SEP Metrics

Fig. 3(a) is a scatter plot for perfect selection verification of the simulated average SEP $P_e(\gamma;\mu)$ on the y-axis, and the SEP metric defined in (18), $M_{\text{ver}}(\mu;\gamma)$ on the x-axis, for 800 different signaling assignments. The SNR is fixed at $\gamma = 6$ dB, and the results are for a ULA with $N_t = 8$ and $N_r = 1$. (The total number of assignments is 40 320, which is very large.) The transmit correlation matrix is calculated using the parameters $\Delta = 1/2$, $\sigma_\theta = 30°$, and $\theta_0 = 30°$. The SNR-dependent term $\beta_{\text{ver}}(\gamma)$ is set to unity. Fig. 3(b) is a scatter plot of the average SEP from simulations and the metric $M_{\text{no}-\text{ver}}(\mu;\gamma)$, defined in (24), for no-selection verification. As before, $\beta_{\text{no}-\text{ver}}(\gamma)$ is set to unity.

The monotonic relationship between the metrics and the average SEP is evident from the plots. So long as this all-important monotonic relationship approximately holds, the metric can be used to compare the various signaling assignments and find the optimal one. On account of the approximations made in the derivation of the metrics and simulation noise, the plot displays some scatter, due to which a small uncertainty exists about the exact SEP value. However, it must be noted that the primary region of interest for optimization purposes is the one with lower values for both $P_e(\mu;\gamma)$ and $M_{\text{ver}}(\mu;\gamma)$.

The validity of the approximations was also verified by simulating several systems with different numbers of antennas and spatial correlations. In each case, the plot of the average SEP displayed the desired monotonic relationship with the metrics for both perfect selection verification and no-selection verification. The monotonic relationship holds regardless of the value of $\beta_{\text{ver}}(\gamma)$ or $\beta_{\text{no}-\text{ver}}(\gamma)$, which is a very useful observation. Therefore, we shall set them to 1 henceforth.

Empirically, we have found that the following simplified versions of the above metrics also work well:

$$M_{\text{ver}}(\mu;\gamma) = -\sum_{s\in\mathcal{S}}\sum_{s'\in\mathcal{S}} |r_{ss'}| \left(\frac{\epsilon}{1-\epsilon}\right)^{d\left(\mu(s'),\mu(s)\right)} \quad \text{or}$$

$$M_{\text{ver}}(\mu;\gamma) = \sum_{s\in\mathcal{S}}\sum_{s'\in\mathcal{S}} \exp\left(-|r_{ss'}|\right) \left(\frac{\epsilon}{1-\epsilon}\right)^{d\left(\mu(s'),\mu(s)\right)}$$

$$M_{\text{no}-\text{ver}}(\mu;\gamma) = -\sum_{s\in\mathcal{S}}\sum_{s'\in\mathcal{S}} \text{Re}\{r_{ss'}\} \left(\frac{\epsilon}{1-\epsilon}\right)^{d\left(\mu(s'),\mu(s)\right)} \quad \text{or}$$

$$M_{\text{no}-\text{ver}}(\mu;\gamma) = \sum_{s\in\mathcal{S}}\sum_{s'\in\mathcal{S}} \exp\left(-\text{Re}\{r_{ss'}\}\right) \times \left(\frac{\epsilon}{1-\epsilon}\right)^{d\left(\mu(s'),\mu(s)\right)}.$$

However, in the rest of paper, we shall continue to use the metric expressions derived earlier.

D. Robustness of Optimal Signaling Assignment

The metrics defined in (18) and (24) depend on system parameters such as the feedback BER, ϵ, and the transmit correlation, $\mathbf{R}_t$. We now make some statements about the robustness of the optimal signaling assignment to changes in these parameters. These give us an idea of whether the optimal signaling assignment can be computed offline, or whether it is so sensitive to the system parameters that it needs to be recomputed in real time whenever the parameters change.

Lemma 1: For small feedback BER $\epsilon \ll 1$, the optimal signaling assignments μ^*_{ver} and $\mu^*_{\text{no}-\text{ver}}$ are independent of ϵ.

Proof: Let $\hat{\mathcal{S}}_{\mathbf{s}}(\mu)$ denote the set of all transmit-antenna indices whose codewords are just 1 bit apart from the codeword $\mu(\mathbf{s})$. Hence, $\hat{\mathcal{S}}_{\mathbf{s}} \triangleq \{s' | s' \in \mathcal{S} \text{ and } d(\mu(\mathbf{s}'),\mu(\mathbf{s})) = 1\}$. When

$\epsilon \ll 1$, single bit errors are most likely. Therefore, the metrics simplify to

$$M_{\text{ver}}(\mu;\gamma) = \frac{\epsilon}{1-\epsilon}\sum_{s\in\mathcal{S}}\sum_{s'\in\hat{\mathcal{S}}_s(\mu)} \exp\left(-\beta(\gamma)|r_{ss'}|^2\right) + o(\epsilon) \tag{25}$$

and

$$M_{\text{no-ver}}(\mu;\gamma) = \frac{\epsilon}{1-\epsilon}\sum_{s\in\mathcal{S}}\sum_{s'\in\hat{\mathcal{S}}_s(\mu)} Q\left(\beta(\gamma)\text{Re}\{r_{ss'}\}\right) + o(\epsilon) \tag{26}$$

where $\lim_{\epsilon\to 0} o(\epsilon)/\epsilon = 0$. Therefore, for $\epsilon \ll 1$, the metrics depend on ϵ only through the common term $\epsilon/(1-\epsilon)$, which implies that the optimal signaling assignments are independent of ϵ [30]. ■

For perfect selection verification, the absolute value of the complex spatial correlation coefficient matters, and not its phase. While a different angle spread and a different mean AoD changes the value of the correlation, the antennas that are farther apart typically have a smaller absolute value of correlation than antennas that are closer. Therefore, the optimal signaling assignment derived for one set of parameters will perform well, even under a different set of parameters.

IV. Signaling Design: Optimization Algorithm

The analysis in the previous section derived closed-form approximations for the average data SEP. The functional forms of $M_{\text{ver}}(\mu;\gamma)$ and $M_{\text{no-ver}}(\mu;\gamma)$ make them amenable to optimization using the binary switching algorithm (BSA), which was invented in early source coding literature on vector quantization over noisy channels [30]. The BSA has recently also been successfully applied to other topics such as bit-interleaved coded modulation [31], [32].

The BSA searches and finds a locally optimal signaling assignment in the set of all assignments, $\mathcal{M}_L$. To run BSA, we need to define the cost function for every signaling assignment for each of the N_t transmit-antenna choices; the total cost is the sum of the costs of all choices. In our problem, the total cost is defined as $M(\mu;\gamma)$, where $M(\mu;\gamma) \triangleq M_{\text{no-ver}}(\mu;\gamma)$ for no-selection verification and $M(\mu;\gamma) \triangleq M_{\text{ver}}(\mu;\gamma)$ for perfect selection verification. From Sections III-A and III-B, the cost for each choice, $s \in \mathcal{S}$, must be defined as

$$\hat{M}_s(\mu;\gamma) = \sum_{s'\in\mathcal{S}} \exp\left(-\beta(\gamma)|r_{ss'}|^2\right)\left(\frac{\epsilon}{1-\epsilon}\right)^{d\left(\mu(s),\mu(s')\right)} \tag{27}$$

for perfect selection verification, and

$$\hat{M}_s(\mu;\gamma) = \sum_{s'\in\mathcal{S}} Q\left(\beta(\gamma)\text{Re}\{r_{ss'}\}\right)\left(\frac{\epsilon}{1-\epsilon}\right)^{d\left(\mu(s),\mu(s')\right)} \tag{28}$$

for no-selection verification. Clearly, we have $M(\mu;\gamma) = \sum_{s\in\mathcal{S}} \hat{M}_s(\mu;\gamma)$. For a detailed description of BSA, the reader is referred to [30].

The key steps of BSA are as follows.

1) Randomly select the initial signaling assignment μ.
2) Calculate the cost function $\hat{M}_s(\mu;\gamma)$ for each choice $s \in \mathcal{S}$, and the total cost $M(\mu;\gamma)$.
3) Sort the elements in the set $\{\hat{M}_s(\mu;\gamma)|s \in \mathcal{S}\}$ in increasing order.
4) Switch the choice with the highest cost with every other choice. Each switch changes μ to a different signaling assignment μ'. For each switch, calculate the new total cost $M(\mu';\gamma)$.
5) Pick the switch with the lowest total cost. If it is lower than the initial total cost, save the corresponding signaling assignment, and return to step 2. If it is higher than the initial total cost, proceed to 6.
6) Switch the choice with the second highest cost with every other choice, and calculate the total cost for each switch.
7) Pick the switch with lowest total cost. If this total cost is lower than the initial cost, save the corresponding signaling assignment, and return to 2. Else, if the total cost is higher than the initial total cost, stop.

The BSA is guaranteed to stop, and it converges to a locally optimum signaling assignment in many cases. To find the global optimum, the algorithm is started with several different initial signaling assignments, and the assignment with the lowest total cost is chosen. The complexity of BSA is of the order of N_t^3. The complexity can be reduced to $N_t^2\log_2(N_t)$ for $\epsilon \ll 1$, when only single feedback bit errors are very likely [30].[6]

We illustrate this with a toy example of a ULA with $N_t = 4$, $\Delta = 0.5$, $\sigma_\theta = 30°$, and $\theta_0 = 30°$. The receiver has $N_r = 1$ antenna and does perfect selection verification. The transmit correlation matrix is $\mathbf{R}_t = [1, -0.60-0.43\mathbf{i}, 0.36+0.34\mathbf{i}, -0.28-0.28\mathbf{i}; -0.60+0.43\mathbf{i}, 1, -0.60-0.43\mathbf{i}, 0.36+0.34\mathbf{i}; 0.36-0.34\mathbf{i}, -0.60+0.43\mathbf{i}, 1, -0.60-0.43\mathbf{i}; -0.28+0.28\mathbf{i}, 0.36-0.34\mathbf{i}, -0.60+0.43\mathbf{i}, 1]$, where $\mathbf{i} = \sqrt{-1}$. Let the initial signaling assignment be 2 3 4 1, which means that the bit sequence 01 (2) signals transmit antenna 1, 10 (3) signals antenna 2, 11 (4) signals antenna 3, and 00 (1) signals antenna 4. From (27), the cost for each choice is $\hat{M}_1(\mu;\gamma) = 0.370$, $\hat{M}_2(\mu;\gamma) = 0.369$, $\hat{M}_3(\mu;\gamma) = 0.369$, and $\hat{M}_4(\mu;\gamma) = 0.370$. The total cost is $M(\mu;\gamma) = 1.478$. Antenna 4 has the highest cost (so does antenna 1). The codeword assigned to antenna 4 is switched with each of the three antenna choices. This gives three new signaling assignments, 2 1 3 4, 2 3 1 4, and 1 3 4 2, with costs 1.477, 1.478, and 1.476, respectively. This process is repeated, and finally finds that the optimal assignment 1 3 4 2 has the lowest cost of 1.476. Note that the optimal assignment need not be unique.[7]

V. Antenna Selection-Verification Methods

We now discuss several antenna selection-verification algorithms that are tailored to the knowledge available at the receiver and attempt to achieve the performance of perfect selection verification. These fall into two categories: blind antenna-selection

[6]The metrics we developed also enable a general formulation based on a combinatorial optimization problem called the quadratic assignment problem (QAP) [33], [34], which tries to find the permutation that minimizes a cost function of the form $\min_{\mu\in\mathcal{M}_L}\sum_{i\in\mathcal{Z}}\sum_{j\in\mathcal{Z}} f_{ij}g_{\mu(i)\mu(j)}$, where $\mathcal{M}_L$ is the set of all possible permutations of the set $\mathcal{Z} = \{1, 2, \ldots, L\}$. Therefore, efficient algorithms developed for QAP can now be applied to our problem, as well.

[7]For example, swapping the zeros and ones in the feedback codewords results in a different signaling assignment with the same performance.

verification, in which there is no additional side information available at the receiver, and nonblind antenna-selection verification, in which additional side information is available.

A. Blind Antenna-Selection Verification

A blind antenna-selection verification receiver detects the transmitted symbol as well as the antenna used to transmit it from the received data only. In addition, the receiver also has access to the *a priori* information of which antenna it asked the transmitter to use. Therefore, the following detection rule minimizes the SEP:

$$\hat{\mathbf{x}} = \arg\max_{x} \{\Pr(x|\mathbf{y}, s, \mathbf{H})\} = \arg\max_{x} \{p(\mathbf{y}|x, s, \mathbf{H})\} \tag{29}$$

where the last step follows because all candidates of x are equiprobable and are independent of s and $\mathbf{H}$. The previous equation can be simplified as

$$\hat{x} = \arg\max_{x} \left\{ \sum_{s'} p(\mathbf{y}|x, s', s, \mathbf{H}) \Pr(s'|s) \right\} \tag{30}$$

$$= \arg\max_{x} \left\{ \sum_{s'} p(\mathbf{y}|x, \mathbf{h}_{s'}) \Phi\left(d\left(\mu(s), \mu(s')\right)\right) \right\}. \tag{31}$$

Equation (30) follows from (29) because the feedback errors are independent of the forward-link channel state. In (31), we used the fact that given $\mathbf{h}_{s'}$, $\mathbf{y}$ is independent of s and $\mathbf{H}$. We shall refer to the receiver based on (31) as the *blind optimal symbol-level selection-verification receiver*. Note that it considers all the possible choices of transmit antennas, and does not determine $\hat{s}$ as an intermediate step. Therefore, the verification-related probabilities $P^{(E)}$ and $P^{(M)}$, defined in (4) and (5), respectively, are not applicable here.

The term $p(\mathbf{y}|x, \mathbf{h}_{s'})$ in (31) is an exponential term, as it is a Gaussian pdf. By using the approximation $\log(\sum_i e^{a_i}) \approx \max_i\{a_i\}$, (31) can be further simplified to[8]

$$\{\hat{x}; \hat{s}\} = \arg\max_{x;s'} \left\{ -\|\mathbf{y} - \mathbf{h}_{s'} x\|^2 + \log \Phi\left(d\left(\mu(s), \mu(s')\right)\right) \right\} \tag{32}$$

where $\hat{s}$ is the transmit antenna assumed by the receiver for data estimation. Taking the logarithm also avoids numerical overflow and underflow problems. The receiver based on (32) shall be called the *blind suboptimal symbol-level selection-verification receiver*. The results show that the performance penalty due to this approximation is extremely negligible. Therefore, we do not distinguish between the two henceforth.

The number of possibilities to be considered by the antenna-verification receiver in (31) and (32) is $4N_t$ because the QPSK constellation consists of four symbols and the number of possible choices of transmit antennas is N_t. For $\epsilon \ll 1$, this complexity can be reduced by only searching over the most probable set of s'. This set corresponds to antennas with codewords that differ from the codeword $\mu(s)$ by only 1 bit. The number of possibilities then reduces to $4\lceil \log_2 N_t \rceil$.

The selection-verification algorithm above is optimal only if the channel changes from one symbol transmission to another. If the channel is block-fading and remains constant over at least $K > 1$ transmissions, the antenna selection-verification performance can be improved by doing it on a block-by-block basis. The optimal receiver now detects the sequence $\{\hat{x}_1, \hat{x}_2, \ldots, \hat{x}_K\}$ as follows:

$$\{\hat{x}_1, \hat{x}_2, \cdots, \hat{x}_K\} = \arg\max_{x_1,\cdots,x_K} \left\{ \sum_{s'} \left[\prod_{i=1}^{K} p(\mathbf{y}_i|x_i, \mathbf{h}_{s'}) \right] \Pr(s'|s) \right\}. \tag{33}$$

As before, (33) can be approximated by

$$\{\hat{x}_1, \hat{x}_2, \cdots, \hat{x}_K; \hat{s}\} = \arg\max_{x_1,\cdots,x_K;s'} \times \left\{ -\sum_{i=1}^{K} \|\mathbf{y}_i - \mathbf{h}_{s'} x_i\|^2 + \log \Phi\left(d\left(\mu(s'), \mu(s)\right)\right) \right\}. \tag{34}$$

We shall refer to the optimal and suboptimal receivers based on (33) and (34), respectively, as *blind block-level selection-verification receivers*. While block-level selection verification outperforms symbol-level selection verification, its complexity grows exponentially with the block-fading length as the number of possibilities is on the order of $4^K N_t$. Therefore, block-level selection verification quickly becomes impractical even for moderate K.

B. Nonblind Antenna Selection-Verification Receiver

While optimal blind selection verification overcomes the catastrophic error-floor limitation of no-selection verification, we shall see that there is still a large performance gap compared with perfect selection verification. In fact, the SEP performance is now limited largely by $P^{(E)}$. Therefore, additional side information is desirable to further reduce the selection-verification error. It can be incorporated into the system by making the transmitter transmit from the *selected* antenna a short pilot symbol sequence before the data.

Let the antenna be selected once every K symbols, where K is smaller than the block-fading duration. Transmission using the selected antenna occurs in two phases: first K_p symbols are used for the pilot; then the remaining $K_d = K - K_p$ symbols are used for data. We also assume that the transmit power can be varied during the two phases. A fraction α of the total energy is allocated to the pilot symbols, and the rest is allocated for data symbols.

In the training phase, the transmitter sends a $1 \times K_p$ pilot symbol vector $\mathbf{x}_p$. The receiver receives

$$\mathbf{Y}_p = \mathbf{h}_{s'} \mathbf{x}_p + \mathbf{W}_p \tag{35}$$

where $\mathbf{W}_p$ is the $N_r \times K_p$ zero-mean unit-variance AWCGN. Since $\mathbf{x}_p$ is known by the receiver, the optimal rule for $\hat{s}$ is as follows:

$$\hat{s} = \arg\max_{s'} \{\Pr(s'|\mathbf{Y}_p, \mathbf{x}_p, s, \mathbf{H})\} \tag{36}$$

$$= \arg\max_{s'} \{p(\mathbf{Y}_p|\mathbf{x}_p, s, s', \mathbf{H}) \Pr(s'|s)\} \tag{37}$$

$$= \arg\max_{s'} \left\{ -\|\mathbf{Y}_p - \mathbf{h}_{s'} \mathbf{x}_p\|_F^2 + \log \Phi\left(d\left(\mu(s'), \mu(s)\right)\right) \right\}. \tag{38}$$

[8]As the noise is assumed to have unit variance, the term $\|\mathbf{y} - \mathbf{h}_{s'} x\|^2$ is not multiplied with any scaling factor.

TABLE I
BEST SIGNALING ASSIGNMENTS FOUND FOR $N_t = 8$ AND $N_t = 16$ FOR DIFFERENT ANTENNA TOPOLOGIES AND RECEIVER VERIFICATION METHODS

Antenna array	N_t	Scenario	Signaling assignment
ULA	4	No-selection verification ($\mu^*_{\text{no-ver}}$)	4 1 2 3
	4	Perfect selection verification (μ^*_{ver})	1 3 4 2
	8	No-selection verification ($\mu^*_{\text{no-ver}}$)	8 1 6 3 2 7 4 5
	8	Perfect selection verification (μ^*_{ver})	8 4 2 6 5 1 3 7
	16	No-selection verification ($\mu^*_{\text{no-ver}}$)	1 7 9 8 10 16 2 15 6 11 5 12 13 4 14 3
	16	Perfect selection verification (μ^*_{ver})	12 21 16 14 6 8 4 2 1 3 11 9 13 15 7 5
UCA	4	Perfect selection verification (μ^*_{ver})	4 3 1 2
	4	No-selection verification ($\mu^*_{\text{no-ver}}$)	4 3 2 1
	8	Perfect selection verification (μ^*_{ver})	1 6 7 3 8 5 2 4
	8	No-selection verification ($\mu^*_{\text{no-ver}}$)	5 1 2 6 7 3 4 8

Here, (37) follows from Bayes' rule, and $\Pr(s'|s, \mathbf{H}, \mathbf{x}_p) = \Pr(s'|s)$ because the errors on the feedback channel are independent of the forward channel $\mathbf{H}$ and $\mathbf{x}_p$. Equation (38) follows because $p(\mathbf{Y}_p|\mathbf{x}_p, s, s', \mathbf{H}) = p(\mathbf{Y}_p|\mathbf{x}_p, \mathbf{h}_{s'})$.

Once the receiver estimates $\hat{s}$, it uses $\mathbf{h}_{\hat{s}}$ to detect the transmitted data. Keeping in mind the complexity of blind selection verification, it is assumed that the receiver does not use the data signals to refine its selection estimate $\hat{s}$. We will refer to the receiver based on (38) as the *nonblind optimal selection-verification receiver*.

VI. NUMERICAL RESULTS

In the numerical results that follow, the error rate of the feedback channel is $\epsilon = 0.04$. Unless mentioned otherwise, the results are for a ULA with $\Delta = 0.5$, $\sigma_\theta = 30°$, and $\theta_0 = 30°$ (Gaussian angle spectrum). When results for a UCA are shown, the UCA parameters are $\sigma_\theta = 10°$, array wavelength-normalized radius $\Omega = 4$, and $\theta_0 = 30°$ (Laplacian angle spectrum). The BSA is run using 100 initial signaling assignments.

A. *Optimal Signaling Assignments*

Table I lists the best signaling assignments that were found using BSA for perfect selection verification and no-selection verification for $N_t = 8$ and $N_t = 16$ for both the ULA and the UCA antenna topologies. For $N_t = 8$, a brute-force search over the possible 40 320 assignments (for an SNR of 6 dB) confirmed the results. For $N_t = 16$, the total number of signaling assignments for single-antenna selection balloons to $16! = 2.0923 \times 10^{13}$, which is well beyond the brute-force search capabilities of many computers. In the table, the binary codeword 000 is denoted by 1, 001 by 2, and so on. Therefore, when we say that the optimal signaling assignment for perfect selection verification with $N_t = 8$ is "8 4 2 6 5 1 3 7," it means the receiver uses codeword 111 (8) to signal transmit antenna 1, 011 (4) to signal transmit antenna 2, and so on.[9] For perfect selection verification, the optimized mapping turns out to be a Gray mapping, which makes intuitive sense, since the nearest neighbor has the largest correlation. However, not all of the possible Gray mappings are optimal. For no-selection verification, the optimum mapping is not a Gray mapping. For a UCA, a Gray mapping does not always exist. The symbols μ^*_{ver} and $\mu^*_{\text{no-ver}}$ shall henceforth denote the best signaling assignments for perfect selection verification and no-selection verification, respectively.

[9]The antennas are indexed in an anticlockwise manner in the UCA.

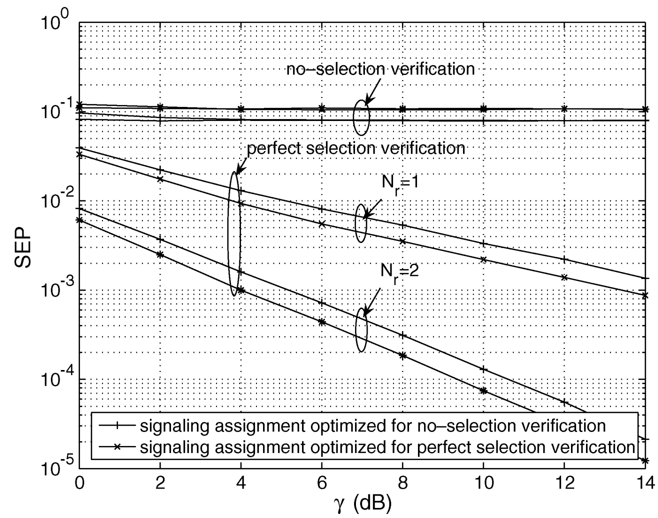

Fig. 4. Average SEP for a ULA for different numbers of receive antennas when the optimal signaling assignments are used with their respective perfect selection verification and no-selection verification receivers. Also shown is the degradation when the signaling assignment optimized for perfect selection verification is used with a no-selection verification receiver, and vice versa ($N_t = 8$).

Fig. 4 compares the data SEP of signaling assignments μ^*_{ver} and $\mu^*_{\text{no-ver}}$ (see Table I), when they are used with the receivers they were optimized for, i.e., perfect selection verification and no-selection verification, respectively. Also shown is the case when μ^*_{ver} is used with a no-selection verification receiver, and vice versa. It is interesting to note that the signaling assignment μ^*_{ver}, optimized for perfect selection verification, performs poorly when used with no-selection verification, and vice versa. Not shown in the figure are the SEP curves for many other randomly generated signaling assignments. These were found to lie in between the two. Optimal signaling lowers the error floor for no-selection verification, and improves the SNR by 1.5–2 dB for perfect selection verification (which does not suffer from an error floor). Increasing the number of receive antennas reduces the SEP considerably for perfect selection verification; however, its impact is minor for no-selection verification. The optimal signaling assignments remain the same for all N_r.

Fig. 5 looks at the UCA with $N_t = 8$ and $N_r = 1$, and compares the data SEP of the optimized signaling assignments (see Table I) and some randomly selected assignments. The optimized assignment results in more than a 0.5 dB gain.

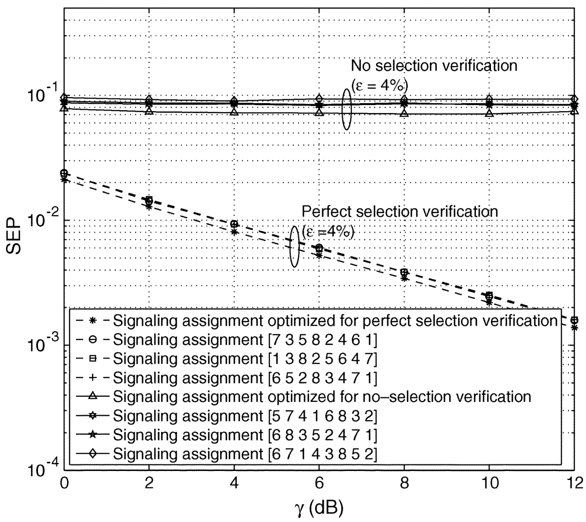

Fig. 5. Average SEP for UCA when μ^*_{ver} is used with perfect selection verification and $\mu^*_{\text{no-ver}}$ is used with no-selection verification. Also shown is the higher average SEP of three randomly generated signaling assignments. ($N_t = 8$, $N_r = 1$, and $\epsilon = 4\%$).

B. Blind Symbol-Level Selection Verification

Fig. 6(a) compares the SEP performance of the blind optimal symbol-level selection-verification receiver and the blind suboptimal symbol-level selection-verification receiver for the two signaling assignments μ^*_{ver} and $\mu^*_{\text{no-ver}}$. It can be seen that there is no difference in SEP performance for these two receivers. For blind symbol-level selection verification, $\mu^*_{\text{no-ver}}$ works better at low SNR, while μ^*_{ver} works better at high SNR.

To understand the behavior of blind symbol-level selection verification, Fig. 6(b) plots its $P^{(E)}$ and $P^{(M)}$ using the signaling assignment μ^*_{ver}. It can be seen that $P^{(E)}$ decreases as the SNR increases and is always below the feedback codeword error probability, which approximately equals $\epsilon \log_2(N_t)$ for $\epsilon \ll 1$. This implies that the performance of the selection-verification algorithm improves with the SNR. On the other hand, $P^{(M)}$ increases with the SNR. This is because at low SNR, when blind selection verification is difficult, the optimal estimate of the transmit antenna is often the one requested by the receiver. At high SNR, when the receiver can accurately determine which transmit antenna was used, $P^{(M)}$ reduces to the probability that $s' \neq s$, which equals $\epsilon \log_2(N_t)$. Therefore, blind suboptimal selection verification behaves like no-selection verification at low SNR and as perfect selection verification at high SNR. Given that the signaling assignment optimized for one receiver is ill-suited for the other, the average SEP curves for the two signaling assignments cross. Thus, for the blind selection verification, the optimal signaling assignment depends on γ.

C. Blind Block-Level and Nonblind Selection Verification

Fig. 7 compares the average SEP of blind symbol-level and block-level selection verification with nonblind selection verification and the ideal perfect selection verification. The ULA has $N_t = 8$ transmit antennas with $N_r = 1$ receive antennas and a block-fading duration of $K = 20$ symbols. The signaling assignment used is μ^*_{ver} for $N_t = 8$ (see Table I). For block-level selection verification, joint detection is over two symbols. Blind block-level selection verification results in a 3 dB gain in the average SEP curves over symbol-level selection verification. However, the blind methods just do not work nearly as well as perfect

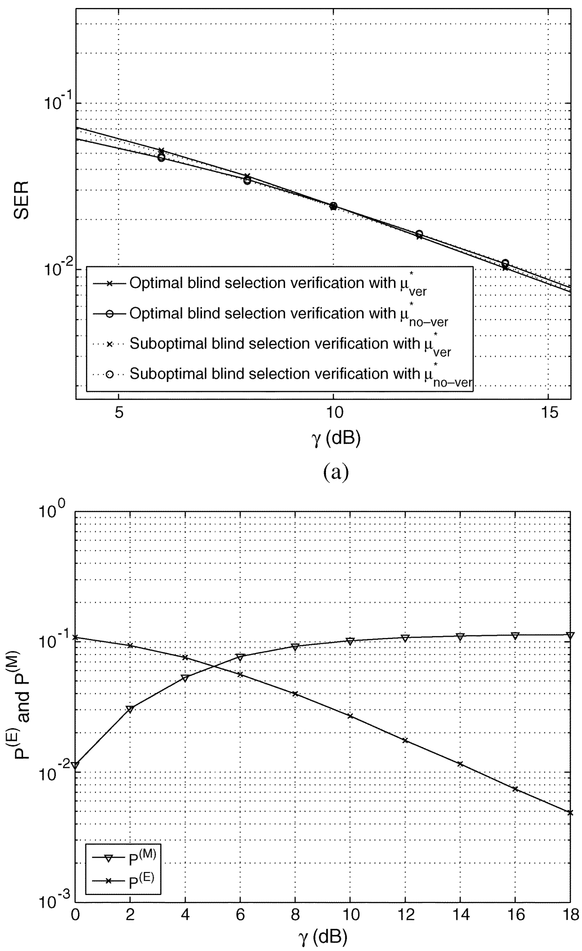

Fig. 6. Average SEP, $P^{(M)}$, and $P^{(E)}$ for blind symbol-level optimal and suboptimal selection-verification receivers. Signaling assignment used is μ^*_{ver} (ULA, $N_t = 8$, and $N_r = 1$. (a) Average SEP. (b) P_M and P_E using μ^*_{ver}.

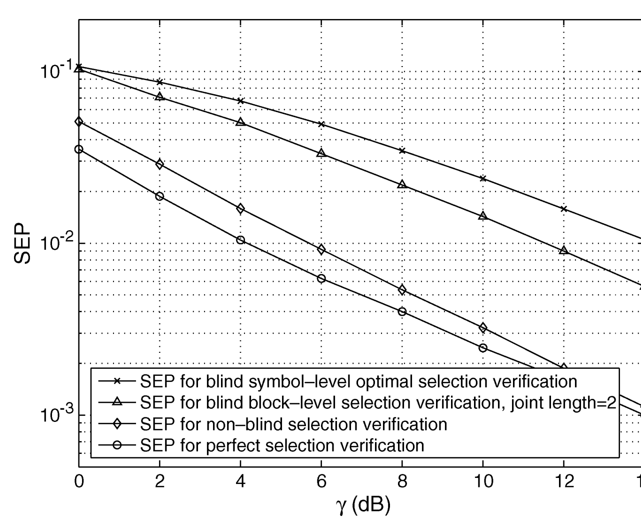

Fig. 7. Comparison of blind and nonblind antenna selection-verification methods. The signaling assignment used is μ^*_{ver} (ULA, $N_t = 8$, $N_r = 1$, $K_p = 1$ symbol, and $K = 20$ symbols).

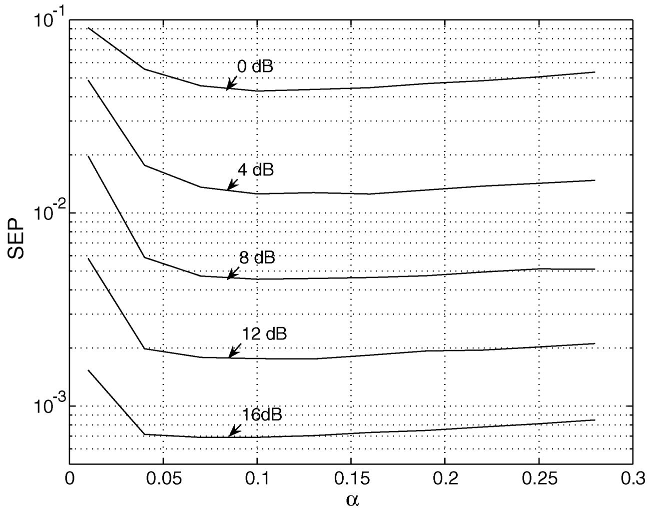

Fig. 8. Optimal amount of side-information. Performance of nonblind optimal antenna selection verification for different data SNRs as a function of α (side-information overhead) with μ^*_{ver} as the signaling assignment (ULA, $N_t = 8$, $N_r = 1$, and $K = 21$ symbols).

selection verification. Side information is one way of bridging this gap. Fig. 7 shows the SEP performance of a nonblind selection verification method that uses one pilot symbol $K_p = 1$ (which is followed by 19 data symbols). The powers for the pilots and data are the same. Even with a small 5% pilot symbol overhead, nonblind selection verification comes close to perfect selection verification.

1) Optimal Side Information Overhead: More symbols or more energy can be allocated to the pilot to improve the selection-verification accuracy. However, increasing the number of pilot symbols reduces the transmission time for data and reduces the net transmission rate. Equivalently, for a fixed total energy budget and a fixed number of pilot symbols, increasing the energy for pilots reduces the energy available for data transmission, and increases the SEP.

Fig. 8 analyzes this tradeoff between side-information overhead and selection verification accuracy. The SEP with nonblind antenna selection verification is plotted for different α and at different SNRs. The parameters assumed are $N_t = 8$ and $N_r = 1$, with $K = 21$ and $K_p = 1$. As before, the signaling assignment μ^*_{ver} is used. The key conclusion is that an optimal tradeoff does exist, and the optimal value of the side information overhead, α, is insensitive to the SNR.

VII. Conclusions

The feedback signaling design matters when the feedback channel used by the receiver to inform the transmitter about which antennas to use is error-prone. For a system that selects one antenna for transmission and uses QPSK modulation, we developed and justified approximate closed-form expressions (metrics) for the average SEP of data with an arbitrary number of receive antennas. The metrics depend on whether no-selection verification or perfect selection verification is used. These were used to systematically find the optimal signaling assignments using the binary switching algorithm. The optimal signaling assignments do not depend on the feedback error probability if it is small, and are independent of the number of receive antennas.

An equally important problem is how the receiver allows for the possibility of feedback errors when it decodes the received data signal. We developed symbol-level and block-level, optimal and suboptimal, blind and nonblind selection-verification methods. The performance gap between blind selection verification and perfect selection verification is quite large, suggesting that nonblind selection, which uses additional side information, e.g., from pilots embedded in the data, is essential in practical implementations of TAS. The optimal amount of side-information overhead was found to be independent of the forward-link SNR.

The feedback signaling problem naturally arises even in a more general set up in which a subset of antennas is selected, and spatial multiplexing or spatial diversity techniques are used in conjunction with higher order modulation and coding. The key issue then becomes one of deriving appropriate optimization-friendly closed-form approximations (or exact solutions) to the resultant SEP. The optimization framework developed in this paper and the selection-verification methods can then be applied directly to handle this.

References

[1] M. Z. Win and J. H. Winters, "Analysis of hybrid selection/maximal-ratio combining in Rayleigh fading," *IEEE Trans. Commun.*, vol. 47, no. 12, pp. 1773–1776, Dec. 1999.

[2] A. F. Molisch, M. Z. Win, and J. H. Winters, "Capacity of MIMO systems with antenna selection," in *Proc. IEEE Int. Conf. Commun.*, Helsinki, Finland, 2001, pp. 570–574.

[3] R. W. Heath, S. Sandhu, and A. Paulraj, "Antenna selection for spatial multiplexing systems with linear receivers," *IEEE Commun. Lett.*, vol. 5, no. 4, pp. 142–144, Apr. 2001.

[4] D. A. Gore and A. Paulraj, "MIMO antenna subset selection with space-time coding," *IEEE Trans. Signal Process.*, vol. 50, no. 10, pp. 2580–2588, Oct. 2002.

[5] A. Ghrayeb and T. M. Duman, "Performance analysis of MIMO systems with antenna selection over quasi-static fading channels," *IEEE Trans. Veh. Technol.*, vol. 52, no. 2, pp. 281–288, Mar. 2003.

[6] Z. Chen, J. Yuan, and B. Vucetic, "Analysis of transmit antenna selection/maximal-ratio combining in Rayleigh fading channels," *IEEE Trans. Veh. Technol.*, vol. 54, no. 4, pp. 1312–1321, Jul. 2005.

[7] S. Thoen, L. Van der Perre, B. Gyselinckx, and M. Engels, "Performance analysis of combined transmit-SC/receive-MRC," *IEEE Trans. Commun.*, vol. 49, no. 1, pp. 5–8, Jan. 2001.

[8] A. F. Molisch and M. Z. Win, "MIMO systems with antenna selection," *IEEE Microw. Mag.*, vol. 5, pp. 46–56, Mar. 2004.

[9] S. Sanayei and A. Nosratinia, "Antenna selection in MIMO systems," *IEEE Commun. Mag.*, vol. 42, pp. 68–73, Oct. 2004.

[10] N. B. Mehta and A. F. Molisch, "Antenna selection in MIMO systems," in *MIMO System Technology for Wireless Communications*, G. Tsulos, Ed. Boca Raton, FL: CRC, 2006, ch. 6.

[11] 3rd Generation Partnership Project, "Physical layer procedures (FDD)," Tech. Rep. 25.214, 2005.

[12] A. F. Molisch, M. Z. Win, and J. H. Winters, "Reduced-complexity transmit/receive-diversity systems," *IEEE Trans. Signal Process.*, vol. 51, no. 11, pp. 2729–2738, Nov. 2003.

[13] D. A. Gore, R. U. Nabar, and A. Paulraj, "Selecting an optimal set of transmit antennas for a low rank matrix channel," in *Proc. ICASSP*, May 2000, pp. 2785–2788.

[14] R. Narasimhan, "Spatial multiplexing with transmit antenna and constellation selection for correlated MIMO fading channels," *IEEE Trans. Signal Process.*, vol. 51, no. 11, pp. 2829–2838, Nov. 2003.

[15] A. F. Molisch, *Wireless Communications*. New York: Wiley/IEEE Press, 2005.

[16] O. Oyman, R. U. Nabar, H. Bolcskei, and A. J. Paulraj, "Characterzing the statistical properties of mutual information in MIMO channels," *IEEE Trans. Signal Process.*, vol. 51, no. 11, pp. 2784–2795, Nov. 2003.

[17] J. P. Kermoal, L. Schumacher, K. I. Pedersen, P. E. Mogensen, and F. Frederiksen, "A stochastic MIMO radio channel model with experimental validation," *IEEE J. Sel. Areas Commun.*, vol. 20, no. 8, pp. 1211–1226, Aug. 2002.

[18] D.-S. Shiu, G. J. Foschini, M. J. Gans, and J. M. Kahn, "Fading correlation and its effect on the quality of multielement antenna systems," *IEEE Trans. Commun.*, vol. 48, no. 5, pp. 502–513, May 2000.

[19] D. Asztely, "On antenna arrays in mobile communication systems: Fast fading and GSM base station receiver algorithms," Royal Inst. Technol., Tech. Rep. IR-S3-SB-9611, Mar. 1996.

[20] W. H. Wong and E. G. Larsson, "Orthogonal space-time block coding with antenna selection and power allocation," *Electron. Lett.*, vol. 39, pp. 379–381, 2003.

[21] Z. Chen, "Asymptotic performance of transmit antenna selection with maximal-ratio combining for generalized selection criterion," *IEEE Commun. Lett.*, vol. 8, no. 4, pp. 247–249, Apr. 2004.

[22] E. N. Onggosanusi, A. Gatherer, A. G. Dabak, and S. Hosur, "Performance analysis of closed-loop transmit diversity in the presence of feedback delay," *IEEE Trans. Commun.*, vol. 49, no. 9, pp. 1618–1630, Sep. 2001.

[23] M. Z. Win and J. H. Winters, "Virtual branch analysis of symbol error probability for hybrid selection/maximal-ratio combining in Rayleigh fading," *IEEE Trans. Commun.*, vol. 49, no. 11, pp. 1926–1934, Nov. 2001.

[24] M. Simon and M.-S. Alouini, *Digital Communications Over Fading Channels*, 2nd ed. New York: Wiley-Interscience, 2005.

[25] R. K. Mallik, "On multivariate Rayleigh and exponential distributions," *IEEE Trans. Inf. Theory*, vol. 49, no. 6, pp. 1499–1515, Jun. 2003.

[26] J.-A. Tsai, R. M. Buehrer, and B. D. Woerner, "Spatial fading correlation function of circular antenna arrays with Laplacian energy distribution," *IEEE Commun. Lett.*, vol. 6, no. 5, pp. 178–180, May 2002.

[27] S. Nagaraj and P. Monogioudis, "Antenna verification for closed loop transmit diversity in UMTS," in *Proc. VTC (Fall)*, Sep. 2004, pp. 3792–3796.

[28] A. Serratore and E. Messina, "Analytical evaluation and performance analysis of antenna verification algorithm in closed loop antenna diversity," in *Proc. Asia-Pacific Conf. Commun.*, Sep. 2003, pp. 9–14.

[29] A. Seeger and M. Sikora, "Antenna weight verification for closed loop transmit diversity," in *Proc. Globecom*, Dec. 2003, pp. 1124–1129.

[30] K. Zeger and A. Gersho, "Pseudo-Gray coding," *IEEE Trans. Commun.*, vol. 38, no. 11, pp. 2147–2158, Nov. 1990.

[31] F. Schreckenbach, N. Gortz, J. Hagenauer, and G. Bauch, "Optimization of symbol mappings for bit-interleaved coded modulation with iterative decoding," *IEEE Commun. Lett.*, vol. 7, no. 12, pp. 593–595, Dec. 2003.

[32] Y. Li and X.-G. Xia, "Constellation mapping for space-time matrix modulation with iterative demodulation/decoding," *IEEE Trans. Commun.*, vol. 53, no. 5, pp. 764–768, May 2005.

[33] P. M. Pardalos, F. Rendl, and H. Wolkowicz, "The quadratic assignment problem: A survey of recent developments," in *Quadratic Assignment and Related Problems*, ser. DIMACS Series in Discrete Mathematics and Theoretical Computer Science, P. Pardalos and H. Wolkowicz, Eds. Providence, RI: American Mathematics Society, 1994, vol. 16, pp. 1–42.

[34] Y. Huang and J. A. Ritcey, "Optimal constellation labeling for iteratively decoded bit-interleaved space-time coded modulation," *IEEE Trans. Inf. Theory*, vol. 51, no. 5, pp. 1865–1871, May 2005.

Yabo Li (S'05) received the B.S. and M.S. degrees in electrical engineering from Xi'an Jiaotong University, Xi'an, China, in 1998 and 2001, respectively, and the Ph.D. degree in electrical engineering from the University of Delaware, Newark, in 2005.

He was a Member of Technical Staff with Bell Labs (Beijing), Lucent Technologies (China), Beijing, China, from July 2001 to July 2002, and an Intern with Mitsubishi Electric Research Labs, Cambridge, MA, from January 2005 to June 2005. He is now with the CDMA system design group of Nortel Networks, Richardson, TX. His research interests include wireless communications, digital signal processing, and information theory.

Neelesh B. Mehta (S'98–M'01–SM'06) received the Bachelor of Technology degree in electronics and communications engineering from the Indian Institute of Technology, Madras, India, in 1996, and the M.S. and Ph.D. degrees in electrical engineering from the California Institute of Technology, Pasadena, in 1997 and 2001, respectively.

He was a visiting graduate student researcher at Stanford University, Stanford, CA, in 1999 and 2000. He was a Research Scientist at the Wireless Systems Research group, AT&T Laboratories, Middletown, NJ, until 2002. In 2002 and 2003, he was a Staff Scientist with Broadcom Corp., and was involved in GPRS and EDGE cellular handset development. Since September 2003, he has been a Member of Technical Staff at the Mitsubishi Electric Research Laboratories, Cambridge, MA. His research includes work on link adaptation, multiple-access protocols, WCDMA downlinks, system-level analysis and simulation of cellular systems, MIMO and antenna selection, and cooperative communications. He is also actively involved in the radio access network physical layer (RAN1) standardization activities in 3GPP.

Andreas F. Molisch (S'89–M'95–SM'00–F'05) received the Dipl. Ing., Dr. Techn., and Habilitation degrees from the Technical University Vienna (TU Vienna), Vienna, Austria, in 1990, 1994, and 1999, respectively.

From 1991 to 2000, he was with TU Vienna, becoming an Associate Professor there in 1999. From 2000–2002, he was with the Wireless Systems Research Department, AT&T (Bell) Laboratories Research, Middletown, NJ. Since then, he has been with Mitsubishi Electric Research Labs, Cambridge, MA, where he is now a Distinguished Member of Technical Staff. He is also a Professor and Chairholder for Radio Systems at Lund University, Lund, Sweden. He has done research in the areas of SAW filters, radiative transfer in atomic vapors, atomic line filters, smart antennas, and wideband systems. His current research interests are MIMO systems, measurement and modeling of mobile radio channels, and UWB, and cooperative communications. He has authored, co-authored or edited four books (among them the recent textbook "Wireless Communications, Wiley-IEEE Press), 11 book chapters, some 100 journal papers, and numerous conference contributions.

Dr. Molisch is an Editor of the IEEE TRANSACTIONS ON WIRELESS COMMUNICATIONS, Co-Editor of a special issue on MIMO and smart antennas in the *Journal of Wireless Communications and Mobile Computing*, and Co-Editor of a recent IEEE JOURNAL OF SELECTED AREAS IN COMMUNICATIONS special issue on UWB. He has been member of numerous TPCs, vice chair of the TPC of VTC 2005 spring, and general chair of ICUWB 2006. He has participated in the European research initiatives "COST 231," "COST 259," and "COST 273," where he was Chairman of the MIMO channel working group. He was Chairman of the IEEE 802.15.4a channel model standardization group, and is also Chairman of Commission C (signals and systems) of URSI (International Union of Radio Scientists). He is the recipient of several awards.

Jinyun Zhang (S'86–M'91–SM'04) received the Ph.D. degree in electrical engineering from the University of Ottawa, Ottawa, ON, Canada, in 1991.

Since 2001, she has been the Head and Senior Principal Technical Staff of the digital communications and networking group at Mitsubishi Electric Research Laboratories (MERL), Cambridge, MA. She is leading many new wireless communications and networking research projects that include UWB, ZigBee, wireless sensor networks, MIMO, high-speed WLAN, and next-generation mobile communications. Prior to joining MERL, she worked for Nortel Networks for more than 10 years, where she held engineering and management positions in the areas of digital signal processing, advanced wireless technology development, and optical networks.

Dr. Zhang is an Associate Editor of the IEEE TRANSACTIONS ON BROADCASTING.